

# Inverting Seismic Data with Facies Trends

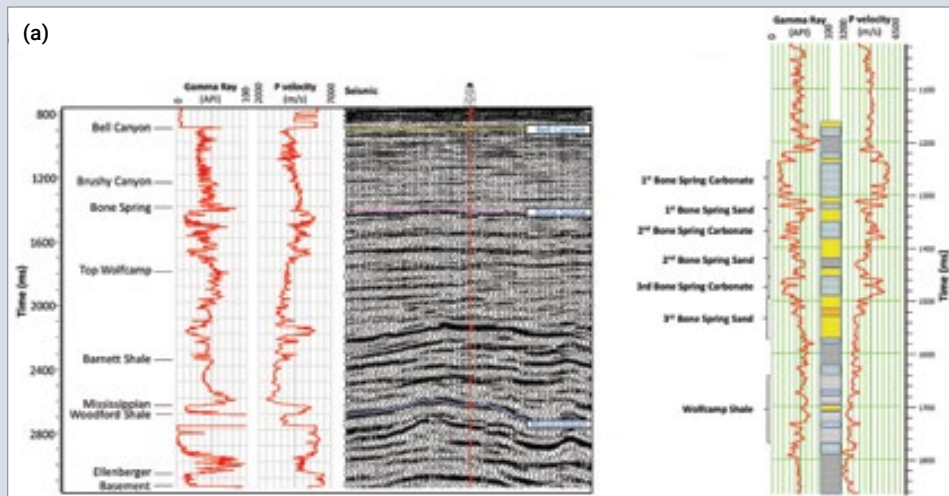


Figure 1: (a) Correlation of well curves for a deep well on 3-D seismic data volume. As the well extends down up to the basement the different litho-units can be read off the formation tops and located on the seismic section. The stratigraphic column of the Delaware Basin focused on the Bone Spring and Wolfcamp intervals and its correlation with seismic data. Data courtesy of TGS, Houston.

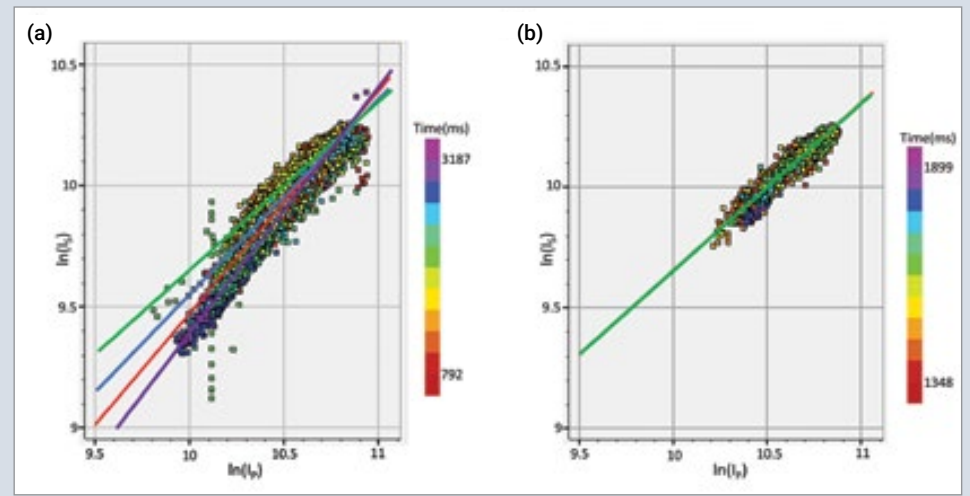


Figure 2: Lithological trend analysis in terms of crossplots to be used in impedance inversion in different litho-intervals. (a) Bell Canyon to Mississippian, (b) Bone Spring top to Top Wolfcamp. The different litho-trends have been overlaid on the one crossplot in (a) with blue line for the Bell Canyon to Bone Spring interval, green for the Bone Spring to Top Wolfcamp interval, and purple line for the Top Wolfcamp to Mississippian interval. Data courtesy of TGS, Houston.

Seismic impedance inversion refers to the transformation of seismic amplitudes into impedance values. Poststack impedance inversion is how the transformation process was first introduced, but it only yields acoustic impedance, which only enables distinction of a target reservoir from the surrounding formations to make a net pay estimation. Prestack simultaneous impedance inversion was introduced at the turn of this century with the objective of characterization of target rock intervals in terms of elastic properties (such as P-impedance, S-impedance, density, VP-VS ratio, Poisson's ratio, Young's modulus,

etc.), which in turn could be associated with petrophysical properties such as porosity, fluid saturation and volume of shale. The authors have written many articles on the different types of impedance inversions and their applications (e.g. see Geophysical Corner in the May, June and July 2015 issues of the EXPLORER).

As seismic data are band-limited, the lack of low frequencies prevents the transformed impedance traces from having the basic impedance or velocity structure (low-frequency trend) crucial to making a geologic interpretation. This low-frequency trend of acoustic impedance is usually derived from well logs or stacking velocities



SHARMA



CHOPRA

and used as a priori information during the inversion process. The workflow generally used for generating the low-frequency trend from a single impedance log or use of a few impedance curves employing

inverse distance-weighted interpolation comes with its own problems that range from not correlating properly at blind well locations or exhibiting artificial tongues with anomalous impedance values, which appear as bull's eyes.

We devised an accurate workflow employing a multilinear regression analysis for building a low-frequency model for impedance inversion that uses both the well log data as well as seismic data. More details on the workflow can be found in the August 2015 Geophysical Corner. Such a low-frequency model helps the impedance inversion process yield a more geological and meaningful impedance transformation.

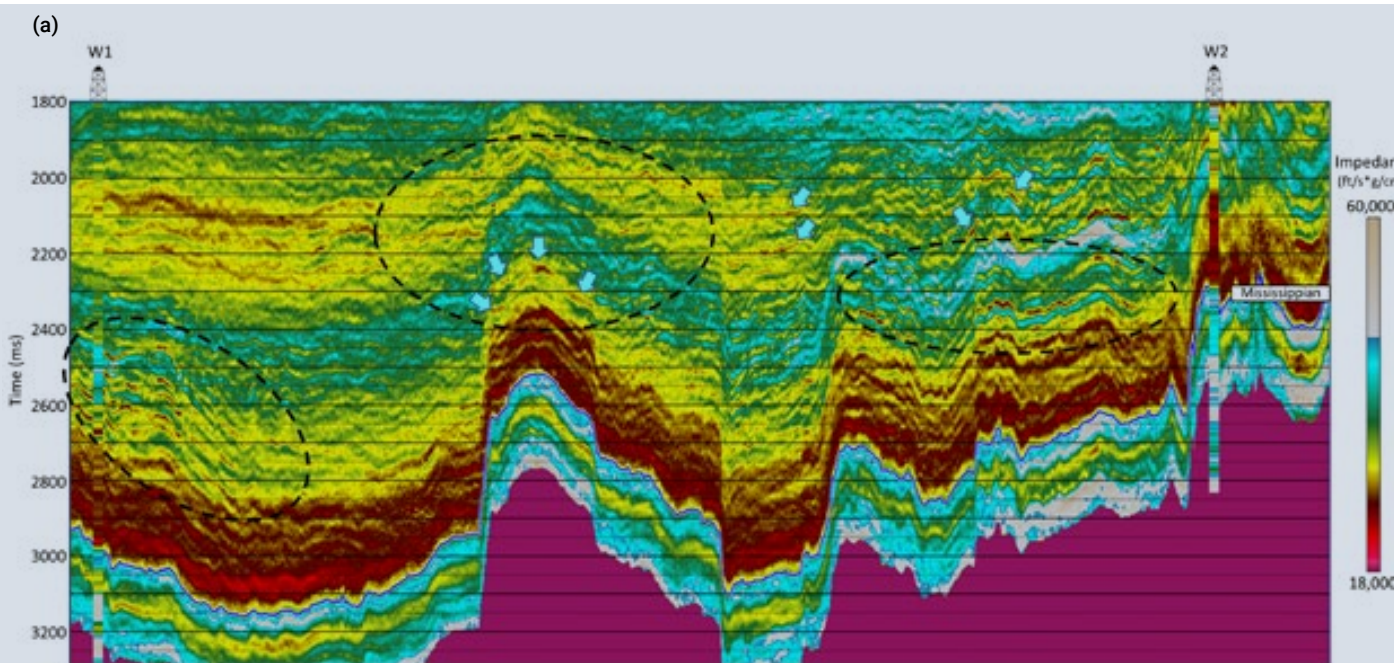
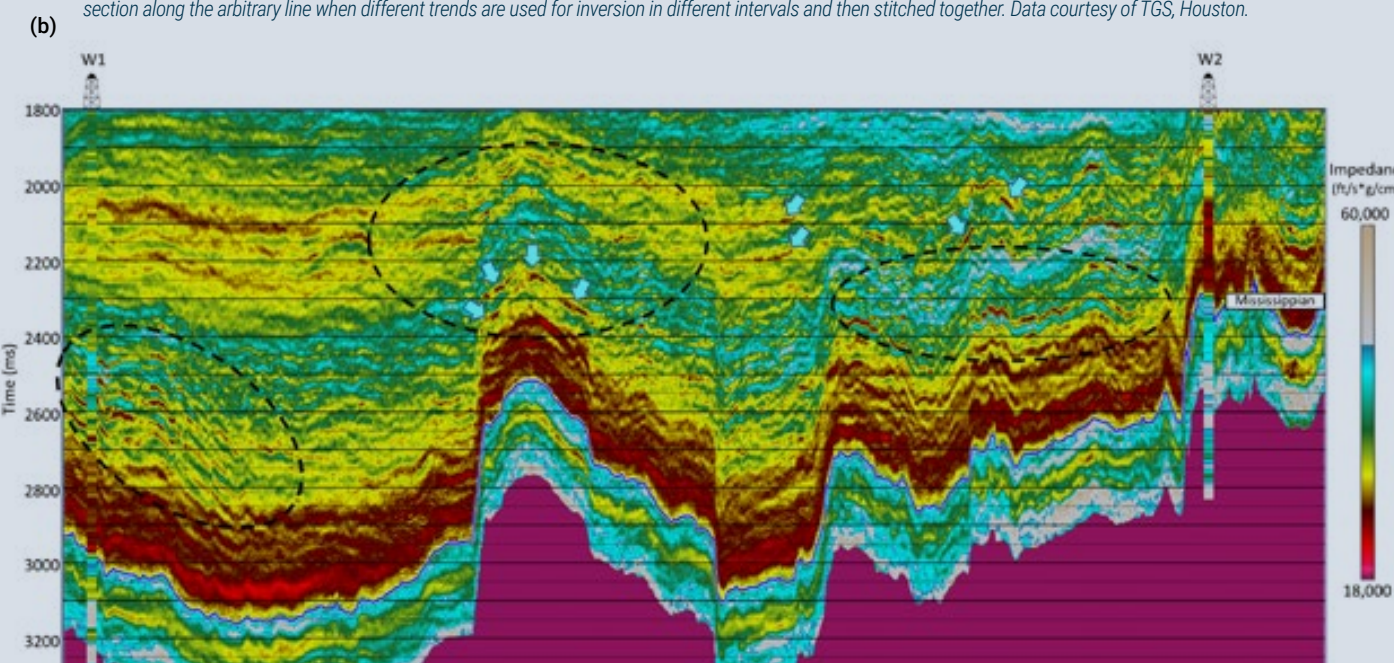


Figure 3 (above): Inverted S-impedance section along the arbitrary line when single trend is used in the inversion analysis. Figure 4 (below): Inverted S-impedance section along the arbitrary line when different trends are used for inversion in different intervals and then stitched together. Data courtesy of TGS, Houston.



## Simultaneous Inversion Workflow

In this article, we show the implementation of a different prestack simultaneous impedance inversion workflow dictated by the complexity of the geologic conditions at hand.

In simultaneous inversion workflow, subsurface low-frequency models for P-impedance, S-impedance and density constrained with appropriate horizons in the broad zone of interest are constructed, and multiple partial angle sub-stacks and the estimated wavelets from each of them are used as input. The output attributes from inversion are P-impedance, S-impedance and density (if the angle of incidence range extends beyond 40 degrees). The inversion process begins with the low-frequency model, which is used to generate synthetic traces for the input partial stack. Zoeppritz equations or their approximations are used to estimate the band-limited elastic reflectivities. These model impedance values are then iteratively tweaked in such a manner that the mismatch between the modeled angle gather and the real angle gather is minimized in a least squares sense. One of the fundamental assumptions made within the simultaneous inversion workflow is the linearization between  $\ln(I_p)$  and  $\ln(I_s)$  as well as  $\ln(I_p)$  and  $\ln(\rho)$ . Such workflows work well for a continuous impedance inversion carried out over a time window, over which the above-mentioned linearity holds.

Quite often, especially when dealing with complex geology, the simultaneous inversion workflow outlined above may not be directly applicable. We cite a case at hand from the Delaware Basin. In figure 1a we show the correlation between the gamma ray and P-velocity well log curves with seismic. The formation tops extend from the Bell Canyon down to the basement. The segment of the lithostrip between the Bone Spring formation and the base of the Wolfcamp formation is shown as zoomed in figure 1b.

See Bone Spring page 25 ►



## Bone Spring from page 22

The Bone Spring formation has sequences of dark grey deep-marine shales interbedded with sands and black carbonates. While the sands were deposited as turbidites during low sea levels, the black bituminous-rich limestones were deposited in deep euxinic basinal environments.


The Wolfcamp formation consists of dark shale and limestone with silt and sand zones. Both the Bone Spring and Wolfcamp are productive formations, as are the Barnett, Mississippian and Woodford intervals. The extent of the broad zone of interest extends from the Bell Canyon (close to 800 milliseconds) to Mississippian (close to 2,800 milliseconds), an overall interval of 2 seconds. Complicating this large time interval for inversion is the fact that it has varied lithology facies in the different subunits. The linearity between  $\ln(I_p)$  and  $\ln(I_s)$  as well as  $\ln(I_p)$  and  $\ln(\rho)$  could be in question, or different facies may exhibit different linear trends. In figure 2a we exhibit a crossplot between  $\ln(I_p)$  and  $\ln(I_s)$  for the complete interval from Bell Canyon to Mississippian, and in figure 2b, another crossplot from Bone Spring top to top of Wolfcamp. A linear trend is seen in the latter. Instead of including more figures, in figure 2a we have overlaid the litho-trend lines from Bell Canyon to Bone Spring (blue line), Bone Spring top to top of Wolfcamp (green line), and top Wolfcamp to Mississippian (purple line). Notice all these facies trends are different, and thus carrying out simultaneous impedance inversion for the 2-seconds long interval with a single trend would not be advisable, to say the least. Consequently, we modified our simultaneous impedance inversion procedure. Instead of carrying out a single inversion run, we performed the inversion in three separate runs, each using its own litho-facies trend

line as discussed above. The three inversion runs were then sutured together as a single impedance volume.

In figures 3 and 4 we show equivalent arbitrary line sections passing through two wells, from the simultaneous impedance inversion run with a single trend (generated for comparison only), and another with three different trends in separate zones and combined. The impedance log curves for the two wells are overlaid on the sections in color. Notice the difference in impedance values in the highlighted zones and at the location of the block arrows. Similar differences were seen on the  $V_p/V_s$  sections as well. Such differences can contribute significantly to the elastic properties which are derived from the P- and S-impedance volumes.

Various commercial impedance inversion software packages have been developed that talk of first deriving depth trends for individual facies in the zone of interest using rock physics analysis, which are then used for impedance inversion.

### Conclusion

We firmly believe that our approach of using an accurate low-frequency model (based on the workflow we follow) as well as using the appropriate lithofacies trends in the simultaneous impedance inversion procedure can bring in accuracy in the desired results. For the exercise at hand, the P-impedance and S-impedance inversion were carried forward into facies computations that were validated with lithology information derived from mudlog cuttings and cores. We will discuss that in another article at a later date. 

*(Editors Note: The Geophysical Corner is a regular column in the EXPLORER, edited by Satinder Chopra, chief geophysicist for TGS, Calgary, Canada, and a past AAPG-SEG Joint Distinguished Lecturer.)*



**AAPG**  
Latin America & Caribbean Region

**SURINAME 2019**  
Geosciences Technology Workshop

## Recent Discoveries and Exploration and Development Opportunities in the Guiana Basin

Torarica Hotel | Paramaribo | 6-7 November 2019

### Session Themes:

- Recent Exploration in Suriname, Guyana and French Guiana
- Maximizing Resource Potential in Emerging Basins
- Enhancing Exploration and Development through Integration and Data Management
- Beyond Guiana: Emerging Plays, Prospects and Discoveries throughout the Caribbean

### Poster Sessions:

- Tectonic Setting & Petroleum Systems of the Guiana Basin
- Tools & Technology to Optimize Exploration & Production

[latinamerica.aapg.org](http://latinamerica.aapg.org)

For information and sponsorship opportunities contact [latinamerica@AAPG.org](mailto:latinamerica@AAPG.org)



## AAPG ROCKY MOUNTAIN SECTION ANNUAL MEETING

LITTLE AMERICA HOTEL, CHEYENNE, WYOMING  
SEPTEMBER 15-18, 2019



## SHORT COURSES

**Hydraulic Fracturing of Horizontal Wells**  
Presenter: Jennifer Miskimins

**Challenges in Horizontal Well Planning and Geosteering**  
Presenters: Andy Finley, Joseph Large, & Jim Suydam

**Multivariate Geostatistical Analysis/ Machine Learning Techniques**  
Presenter: Bill Bashore

**Core Workshop: Comparison of the Mid-Carboniferous Heath and Tyler Intervals, Central Montana to the Williston Basin, North Dakota**  
Presenters: Richard Bottjer, Stephan Nordeng, Timothy Nesheim, & John Curtis

**Sequence Stratigraphy of Unconventional Resource Plays**  
Presenter: Ali Jaffri

**Unconventional Resource Technology**  
Presenters: Andy Finley & Leo Giangiacomo

Photos courtesy of Patrick Amole

Website: <https://rmsaapg2019.com/>